

M(μ -CN)Fe(μ -CN)M' Chains with Phthalocyanine Iron Centers: Redox, Spin-State, and Mixed-Valence Properties

Andreas Geiss, Mario J. Kolm, Christoph Janiak, and Heinrich Vahrenkamp*

Institut für Anorganische und Analytische Chemie der Universität Freiburg, Albertstrasse 21, D-79104 Freiburg, Germany

Received January 31, 2000

Dinuclear complexes with M–CN–ZnPc and M–CN–FePc–CN arrays and trinuclear complexes with M(μ -CN)Fe(μ -CN)M' arrays containing central metal phthalocyaninato (Pc) and external Cp(dppe)Fe or Cp(PPh₃)₂Ru building blocks (M) and having all possible orientations of the bridging cyanide ligands were subjected to electrochemical and preparative redox reactions. The species with unpaired electrons show characteristic MMCT bands in the near-IR spectra, the energies of which depend in a typical fashion on the nature of the building blocks and the orientation of the cyanide bridges and can be correlated with the redox potentials. Cyclic voltammetry has revealed electronic communication between the external organometallic units. An analysis of the MMCT spectra allows the assignment of the odd-electron complexes as class II mixed-valence species. The magnetic moments of the complexes with central Fe(III)Pc units are characteristically higher than the spin-only value for one unpaired electron. A Mössbauer investigation has shown that the M–CN–Fe(III)Pc–NC–M complexes undergo a low-spin-to-high-spin crossover of the Fe(III) component above room temperature.

Ever since the basic work of Henry Taube and his successors on metal-to-metal redox reactions,^{1–4} investigations on metal–metal charge transfer, mixed valence, and spin localization in ligand-linked dinuclear systems have been attractive subjects of study. The linkers mediating electronic or magnetic interactions between the metallic centers may be as simple as an oxygen atom or as sophisticated as a 20-carbon chain.^{4–8} A popular spacer with good electronic “conductance” is the cyanide ion,^{9–12} which, at its carbon and nitrogen termini, has quite different bonding characteristics and, hence, creates a clear differentiation of the two metallic units attached to it. As a consequence, M–CN–M' complexes in the mixed-valence state can hardly be fully delocalized and are at best class II mixed-valence species according to the Robin and Day classification.¹³

The situation should be different in symmetrical trinuclear complexes of the type M(μ -CN)M'(μ -CN)M. Here, the outer metal M units can be in identical electronic situations and are hence amenable to a mixed-valence state where the interacting centers are up to 10 Å apart. We, among others,¹² have prepared and fully characterized a series of such complexes.^{14–19} One important finding of our study was that long-range metal–metal

interactions in these systems occur only along linear M'(μ -CN)M(μ -CN)M' arrays, i.e., when the outer metal centers M' are attached trans to the central M center.

The present study extends these investigations. As described in the preceding paper,¹⁹ a central unit comprised of a redox-active metal (Fe) and a redox-active ligand (phthalocyanine, Pc) was cyanide-linked to redox-active organometallic units containing Fe and Ru. Various linkage isomers were obtained, including those with all three possible cyanide orientations in the M'(μ -CN)M(μ -CN)M' array. Thus, quite variable redox chemistry was to be expected, and it seemed attractive to study the possible metal–metal interactions. This paper describes the electrochemical and preparative redox reactions, the MMCT spectroscopy, the magnetic moments, and a Mössbauer investigation of the trinuclear complexes and some dinuclear reference compounds. One of the aims was to identify among the Fe–CN–Fe systems authentic cases of “molecular Prussian Blue”.

Results and Discussion

Compounds under Investigation. The synthesis, isomerization, and full characterization of all di- and trinuclear complexes have been described in the preceding paper.¹⁹ They are listed under a different numbering scheme in this paper for reasons of clarity. Those complexes bearing charges were employed as salts with PPN or SbF₆ counterions. The system of the numbering scheme is as follows:

1. Capital letters (**A**, **B**) identify the external organometallic units Cp(dppe)Fe (**A**) and Cp(PPh₃)₂Ru (**B**).

- (1) Taube, H. *Adv. Inorg. Chem. Radiochem.* **1959**, *1*, 1.
- (2) Taube, H. *Electron Transfer Reactions of Complex Ions in Solution*; Academic Press: New York, 1970.
- (3) Sutin, N. *Acc. Chem. Res.* **1968**, *1*, 225.
- (4) Creutz, C. *Prog. Inorg. Chem.* **1983**, *30*, 1.
- (5) Haim, A. *Prog. Inorg. Chem.* **1983**, *30*, 273.
- (6) Kahn, O. *Adv. Inorg. Chem.* **1995**, *43*, 179.
- (7) Murray, K. S. *Coord. Chem. Rev.* **1974**, *12*, 1.
- (8) Bartik, T.; Bartik, B.; Brady, M.; Dembinsky, R.; Gladysz, J. A. *Angew. Chem.* **1996**, *108*, 467; *Angew. Chem., Int. Ed. Engl.* **1996**, *35*, 414.
- (9) Scandola, F.; Argazzi, R.; Bignozzi, C.; Chiorboli, C.; Indelli, M. T.; Rampi, M. A. *Coord. Chem. Rev.* **1993**, *93*, 1243.
- (10) Balzani, V.; Juris, A.; Venturi, M.; Campagna, S.; Serroni, S. *Chem. Rev.* **1996**, *96*, 759.
- (11) Dunbar, K. R.; Heintz, R. A. *Prog. Inorg. Chem.* **1997**, *45*, 283.
- (12) Vahrenkamp, H.; Geiss, A.; Richardson, G. N. *J. Chem. Soc., Dalton Trans.* **1997**, 3643.
- (13) Robin, M. B.; Day, P. *Adv. Inorg. Chem. Radiochem.* **1967**, *10*, 247.
- (14) Zhu, N.; Vahrenkamp, H. *J. Organomet. Chem.* **1999**, *573*, 67.

- (15) Geiss, A.; Keller, M.; Vahrenkamp, H. *J. Organomet. Chem.* **1997**, *541*, 441.
- (16) Richardson, G. N.; Brand, U.; Vahrenkamp, H. *Inorg. Chem.* **1999**, *38*, 3070.
- (17) Geiss, A.; Vahrenkamp, H. *Eur. J. Inorg. Chem.* **1999**, 1793.
- (18) Richardson, G. N.; Vahrenkamp, H. *J. Organomet. Chem.* **2000**, *593*–594, 44.
- (19) Geiss, A.; Vahrenkamp, H. *Inorg. Chem.* **2000**, *39*, 4029–4036.

2. Lowercase letters (**a**, **b**, **c**) identify the linkage isomers, i.e., the orientation of the two bridging cyanide ligands, as in M–CN–Fe–NC–M (**a**), M–CN–Fe–CN–M (**b**), and M–NC–Fe–CN–M (**c**).

3. Complexes differing only in the oxidation state of the central iron atom have the same number but are differentiated by their charge, as in **3** and **[3]**⁺.

Dinuclear Complexes.



1A, **[1A]**⁺, M = Cp(dppe)Fe; **1B**, **[1B]**⁺, M = Cp(PPh₃)₂Ru



[2A]⁻, **2A**, M = Cp(dppe)Fe; **[2B]**⁻, **2B**, M = Cp(PPh₃)₂Ru

Trinuclear Complexes.



3Aa, **[3Aa]**⁺, M = Cp(dppe)Fe;

3Ba, **[3Ba]**⁺, M = Cp(PPh₃)₂Ru



3Ab, **[3Ab]**⁺, M = Cp(dppe)Fe;

3Bb, **[3Bb]**⁺, M = Cp(PPh₃)₂Ru



3Ac, **[3Ac]**⁺, M = Cp(dppe)Fe

Cp(dppe)Fe–CN–FePc–CN–Ru(PPh₃)₂Cp

4b, **[4b]**⁺

Cp(PPh₃)₂Ru–CN–FePcCN–Fe(dppe)Cp

5b, **[5b]**⁺

Thus, the system under consideration is comprised of 10 redox pairs, i.e., 20 complexes, of which 14 had actually been isolated prior to this investigation.¹⁹

Voltammetry. The redox chemistry of metal phthalocyanines is very well developed. For the FePc system, as a typical example, two 1e reductions of the phthalocyanine ring at strongly negative potentials, one Fe(II)/Fe(III) redox process in the center of the potential range, and one 1e oxidation of the phthalocyanine ring at strongly positive potentials are observed.²⁰ The ZnPc system shows only the two reductions and the one oxidation of the ligand.²¹ The di- and trinuclear complexes of this study could be expected to contribute one or two oxidation steps of the external organometallic units to this. Cyclic voltammograms were recorded to verify this and to gain the first pieces of information on possible electronic interactions between the external metal units. Table 1 lists the data.

The dinuclear reference compounds **1** and **2** provided the assignments of the redox waves that could be used with good reliability for the other complexes: the first reductive wave of the phthalocyanine ring occurs at or beyond the lower end of the measurement window in dichloromethane. The redox wave of the central iron atom is close to 0.0 V vs Ag/AgCl. The oxidation of the Cp(dppe)Fe unit occurs in the 0.5–0.8 V range, and the less electron-rich Cp(PPh₃)₂Ru unit is oxidized in the

Table 1. Cyclic Voltammetry^a

complex pair	Pc ^{3-/2-}	Fe ^{2+/3+}	M ^{2+/3+}	Pc ^{2-/1-}
1A / [1A] ⁺	-1.17	–	0.76	0.43
1B / [1B] ⁺	-1.13	–	1.07	0.46
[2A] ⁻ / 2A	–	-0.06	0.64	0.64
[2B] ⁻ / 2B	–	0.00	1.16	0.75
3Aa / [3Aa] ⁺	–	-0.09	0.67/0.75	1.17
3Ba / [3Ba] ⁺	–	-0.01	1.22/1.31	0.86
3Bb / [3Bb] ⁺	–	0.08	1.11/1.31	0.88
3Ac / [3Ac] ⁺	–	-0.03	0.36/0.51	1.17
4b / [4b] ⁺	–	0.00	0.71/0.90	1.28
5b / [5b] ⁺	–	-0.03	0.50/1.23	0.96

^a Substance dissolved in CH₂Cl₂, half-wave potentials vs Ag/AgCl. The voltammetric traces were identical whether starting from complex No. or **[No.]**⁺.

1.0–1.3 V range. Figure 1 is meant to visualize the quality of the measurements using the simplest compound **1A** as an example.

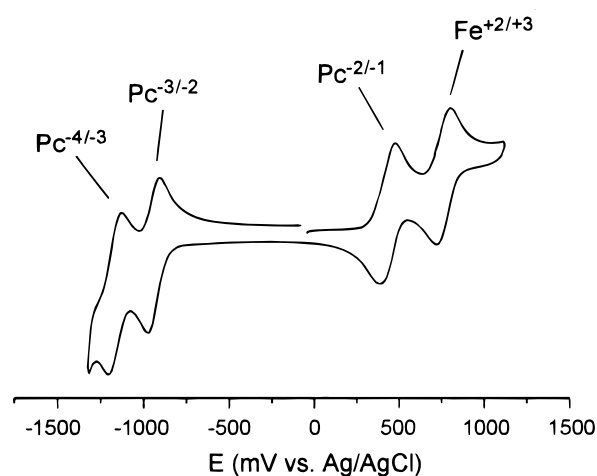


Figure 1. Cyclic voltammogram of **1A** (for details, see Table 1 and Experimental section).

For all trinuclear compounds, the reduction of the phthalocyanine ring occurs outside the potential window, and the redox wave for the central iron atom spans a very narrow potential range of 0.17 V around 0.00 V. This seems to indicate that the FePc unit has quite a balanced electronic situation, irrespective of the kind and orientation of the attached cyanometal units. As discussed in the preceding paper¹⁹ for the $\nu(\text{CN})$ data, the reason for this must be an efficient motion of electron density along the M(μ -CN)FePc(μ -CN)M chains brought about by the σ -donation from the cyanides' N termini and the π -acceptance at the cyanides' C termini. It is noticeable, however, that in each pair of **A** and **B** compounds, the replacement of the Cp(dppe)Fe unit by the less electron-rich Cp(PPh₃)₂Ru unit increases the redox potential of the central Fe by 0.06–0.11 V.

Each of the trinuclear complexes displays two redox waves for the external organometallic units. This is trivial for **4b** and **5b**, which contain two different such units. In the other four cases, however, this is the indication of electronic interaction between the external units. It was to be expected, since the metal–cyanide chains are linear, just as observed before by us for similar arrangements with central PtL₂¹⁶ and Fe(salen) units.¹⁷ The splitting of the redox waves by 0.08–0.20 V is small and not clearly discernible in the cyclic voltammograms. But square-wave voltammograms make it easily visible, as presented in Figure 2 for compounds **3Aa** and **3Ba**. It is similar to or larger than the previously observed splittings^{16,17} and, hence, can be considered typical for two metal atoms separated

(20) Lever, A. B. P.; Wilshire, J. P. *Inorg. Chem.* **1978**, *17*, 1145.

(21) Lever, A. B. P.; Wilshire, J. P. *Can. J. Chem.* **1976**, *54*, 2514.

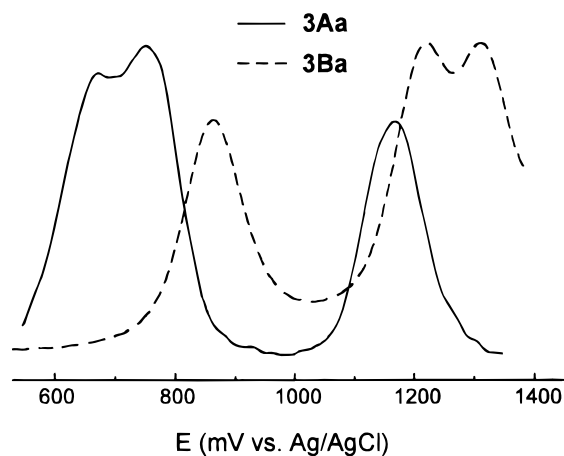


Figure 2. Square wave voltammograms of **3Aa** and **3Ba** (for details, see Table 1 and Experimental section).

by two cyanide bridges, i.e., 10 Å apart. A verification of the long-range metal–metal interactions by MMCT spectroscopy (see below) was impossible. It would have required the preparation of the doubly oxidized compounds containing one of the external metal units and the central iron in the oxidized state. We tried this during the preparative redox investigations, but the desired compounds seem to be chemically unstable.

The values of the redox potentials of the external organometallic units show typical trends. As usual, the Cp(PPh₃)₂Ru units are more difficult by 0.5–0.7 V to oxidize than the Cp(dppe)Fe units in the same environment, reflecting a considerable difference in their electronic situation. Second the typical distinction between C- or N-bound cyanide^{16,17,22} is very visible, unlike in the central FePc unit. The most prominent example for this distinction is the pair of complexes **3Aa** and **3Ac**, where the corresponding redox potentials move by 0.31 and 0.24 V, respectively.

The oxidation step of the phthalocyanine rings occurs at quite variable potentials, cf. Table 1. This can, however, be analyzed in a systematic fashion and is not in contradiction to the fact that the redox potential of the central iron atom varies so little. For this analysis, the complexes can be arranged in groups within which the redox potential of the Pc ring varies only little. The first group is the zinc complexes **1**. They have the lowest redox potential for Pc because its oxidation is not preceded by the oxidation of the central metal atom. The second group is the dinuclear complexes **2**, having an intermediate redox potential for Pc. The third group is the complexes **3B**, having only external ruthenium units. The group is oxidized after the Pc ring; hence, the Pc ring's redox potential is not raised significantly above that of complexes **2**. The fourth group is the complexes **3A**, having only external iron units. The group is oxidized before the Pc ring, whose redox potential is thereby raised significantly due to Coulombic forces. The situation is ambiguous only for the complexes **4b** and **5b**, where the assignments of the 0.9 and 1.2 V steps, respectively, may be exchanged. In all other trinuclear cases, the assignment of the steps is based on the experience that the splitting of the redox waves for the identical external metal units is in the 0.2 V range.^{16,17}

Preparative Redox Reactions. The cyclic voltammograms of all complexes under investigation indicated reversible redox interconversions for the central FePc units. The convenient potential range for these interconversions (near 0 V vs Ag/AgCl)

Table 2. Preparative Redox Reactions^a

oxidation	reduction
CoCp ₂ [2A] → 2A	2A → CoCp ₂ [2A]
CoCp ₂ [2B] → 2B	2B → CoCp ₂ [2B]
3Ba → [3Ba]SbF ₆	[3Ba]SbF ₆ → 3Ba
3Bb → [3Bb]SbF ₆	[3Bb]SbF ₆ → 3Bb
3Ac → [3Ac]SbF ₆	

^a Oxidation with [FeCp₂]SbF₆, reduction with CoCp₂. For details, see Experimental Section.

made it likely that they should work on the preparative scale as well. This could be verified in nine cases using [FeCp₂]SbF₆ for oxidation and CoCp₂ for reduction. The course of the reactions and the persistence of the products in solution could easily be controlled by the intense colors of the metal phthalocyanine complexes: all Fe(III)Pc derivatives are deep blue and all Fe(II)Pc derivatives deep green.

The reactions performed are listed in Table 2. Most of the compounds produced by the interconversions were already obtained in the preceding paper¹⁹ via nonredox routes. Only complex [**3Ac**]SbF₆ (**9c** in the preceding paper) was accessible only by the oxidation of **3Ac**. Also, complexes [**2A**]⁺ and [**2B**]⁺ are not accessible by other means and are described in this paper for the first time as cobalticinium salts resulting from reduction of **2A** and **2B**. The preparation of [**3Ac**]⁺ through oxidation has made possible the detailed study of the cyanide/isocyanide isomerization of [**3Ac**]⁺ via [**3Ab**]⁺ to [**3Aa**]⁺. In several cases, the redox process starting from an easily accessible trinuclear complex was also the better alternative for making its oxidized or reduced analogue, the best example for this being the preparation of **3Ba** by reduction of [**3Ba**]SbF₆ (see Experimental Section) rather than from Fe(II)Pc and Cp(PPh₃)₂Ru–CN.¹⁹

Metal–Metal Charge Transfer. The electronic spectra of all complexes described are dominated by the extremely intense Q-bands of the MPc units in the 660–690 nm range. In addition, all compounds containing Fe(III)Pc show moderate to strong bands near 800 nm and one or two bands in the NIR spectra. Both can be assigned as charge-transfer bands, the 800 nm bands as LMCT from the Pc ligand to Fe(III) and the NIR bands as MMCT from the external metals to Fe(III). The mixed-valence nature of the complexes containing Fe(III)Cp thus corresponds to a short-range MMCT across one cyanide bridge, while a long-range MMCT between the two external metal units would require the existence of the complexes that contain one of these units in the oxidized state. Table 3 lists the spectral data. Figure 3 shows representative spectra for Cp(dppe)Fe-containing compounds. The Supporting Information shows a related figure for a Cp(PPh₃)₂Ru-containing compound.

Table 3. Vis/NIR Data of Trinuclear Complexes Containing Fe(III)Pc {λ_{max} (ε_{max}) [nm (M⁻¹ cm⁻¹)]} in CH₂Cl₂

complex	Q-band	LMCT	MMCT
2A	684(40500)	780(3100)	1180(1400)
2B	684(41300)	782(4050)	850sh(1130)
[3Aa] ⁺	684(46000)	804(3030)	1293(5370)
[3Ba] ⁺	684(46700)	804(6300)	880sh(4430)
[3Ab] ⁺	686	798	1300, 2150 ^a
[3Bb] ⁺	688(44200)	794(4180)	930(2510), 1116(2660)
[3Ac] ⁺	684(46800)	796(3500)	2250(8030)
[4b] ⁺	688(39900)	796(3220)	1323(3260)
[5b] ⁺	684(40700)	798(2950)	890sh(1330), 2200(6710)

^a Extinction coefficients not determined since [**3Ab**]⁺ is a transient species.¹⁹

The NIR data yield an arrangement of the complexes into two groups, those containing Cp(dppe)Fe and those containing

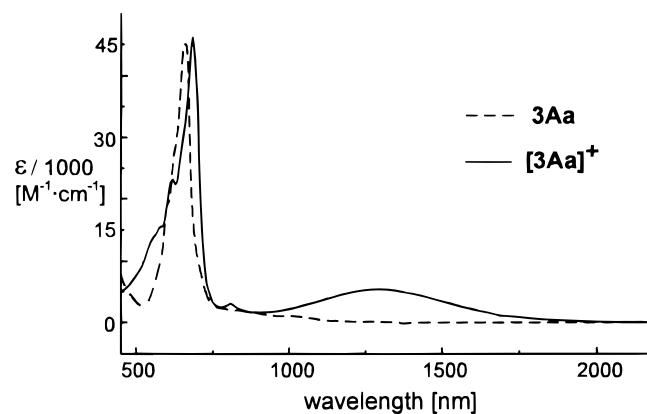


Figure 3. Comparison of the Vis/NIR spectra of trinuclear complexes containing Fe(II)Pc (**3Aa**, dashed line) and Fe(III)Pc (**[3Aa]⁺**, solid line). For details see Table 3.

Cp(PPh₃)₂Ru. In accordance with the fact that the latter is much more difficult to oxidize (cf. the $E_{1/2}$ values for Cp(dppe)Fe–CN (0.48 V) and Cp(PPh₃)₂Ru–CN (0.79 V)), the MMCT bands of the former are located further into the NIR region and are clearly separated from the other bands. The MMCT bands of the Ru-containing species extend into the visible range and, in cases, are somewhat difficult to discern from the other bands because they appear as shoulders only.

A similar relation between the electron richness of the external metal units and the MMCT band positions emerges from the effects of CN/NC isomerism. The complex pair **[3Aa]⁺**/**[3Ac]⁺** (whose NIR spectra are displayed in the preceding paper¹⁹) shows this in the most pronounced way: **[3Aa]⁺** contains Cp(dppe)Fe attached to the cyanide carbon—i.e., electron-poor Fe(II)—and, hence, requires higher energies (lower wavenumbers) for the MMCT process than its isomer **[3Ac]⁺** with N-bound Cp(dppe)Fe. For the same reason, the asymmetrical complexes **[3Ab]⁺** and **[3Bb]⁺** show two MMCT bands resulting from the C-bound and N-bound external metal units. In the complex pair **[4b]⁺**/**[5b]⁺**, this leads to a coincidence: **[5b]⁺** contains N-bound Fe(II) (MMCT at 2240 nm) and C-bound Ru(II) (MMCT at 890 nm), while the inverse situation in **[4b]⁺** shifts both MMCT transitions to the same location at 1323 nm. The latter, in turn, is in accordance with the assignments of the redox potentials for the Fe(II) and Ru(II) units of **4b** and **5b** (cf. Table 1).

As a test for the correlation between the electron richness of the ML_{*n*} units and the MMCT band positions, the redox energies were correlated with the MMCT energies. For this purpose, the redox energies were taken as the difference between the $E_{1/2}$ values for Fe(II)Pc/Fe(III)Pc and Cp(PR₃)₂M(II)/Cp(PR₃)₂M(III) for a given compound and then converted to cm⁻¹ according to $\Delta E_{1/2}(\text{cm}^{-1}) = 8064\Delta E_{1/2}(\text{V})$. Applying this to all redox situations in the trinuclear complexes in Table 3 yielded nine data points (taking into account that the $E_{1/2}$ values for the transient species **[3Ab]⁺** are unknown and that each of the unsymmetrical complexes produces two data points). Figure 4 shows the graph constructed from these points whose regression analysis yields the energy relation

$$\tilde{\nu}_{\text{max}}(\text{cm}^{-1}) = 1.01\Delta E_{1/2}(\text{cm}^{-1}) + 1003$$

The correlation is fair, and the slope of the regression line is close enough to unity to show that the internal redox process—i.e., the MMCT transition—can be quantified on the basis of the external redox data obtained from the voltammetric measurements. This is satisfying, considering Coulombic forces affect the $E_{1/2}$ values for the external metal units, e.g., in some

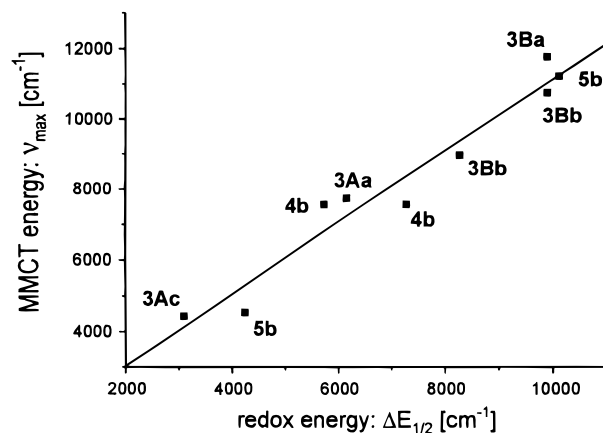


Figure 4. Plot of the MMCT energies vs the redox energies of the trinuclear complexes (for details, see text).

cases the Pc²⁻/Pc⁻ redox process occurs before and, in some cases, after the oxidation of the external metal unit (see above), and likewise in the asymmetrical complexes, the oxidation of the first external metal changes the redox potential of the second.

A semiquantitative treatment of the MMCT data according to the Hush model,²⁴ as applied by others²⁵ and us^{16,22} to di- and trinuclear systems with cyanide bridges, has yielded additional quantitative information on the mixed-valence nature of the trinuclear complexes. Table 4 lists data for the symmetrical complexes as obtained by the procedures outlined at the bottom of the table. As usual for this kind of approximation,^{16,22,25,26} the calculated half-widths of the IT bands are about two-thirds of the observed ones. The reorganization energies are somewhat smaller than those previously observed.^{16,22} The important parameter α^2 , the electron delocalization parameter, results as 0.02–0.04, which is on the same order of magnitude as that found by us for related dinuclear complexes.²² This confirms again that the metal–metal charge transfer in these trinuclear complexes occurs across a single cyanide bridge. In comparison to other dinuclear mixed-valence systems,^{4,13,24} the α^2 values are actually quite high. This justifies the statement that the complexes investigated belong to class II of the mixed-valence compounds according to the classification of Robin and Day.¹³

Table 4. IT Analysis According to the Hush Model

complex	ν_{max} (cm ⁻¹)	$(\Delta\nu_{1/2})_o$ (cm ⁻¹) ^a	ΔE_o (cm ⁻¹) ^b	$(\Delta\nu_{1/2})_c$ (cm ⁻¹) ^a	α^2 ^c	λ_{fc} (cm ⁻¹) ^d
[3Aa]⁺	7730	3190	6160	1910	0.019	1570
[3Ac]⁺	4440	2780	3100	1760	0.043	1350
[3BA]⁺	11760	3860	8690	2540	0.012	3072

^a Observed (o) and calculated (c) half-widths of the MMCT bands: $(\Delta\nu_{1/2})_c = [2300(\nu_{\text{max}} - \Delta E_o)]^{1/2}$. ^b Calculated from the differences of the redox potentials (in V) as $\Delta E_o = 8064\Delta E_{1/2}$. ^c Calculated as $\alpha^2 = 4.24 \times 10^4 [(\epsilon_{\text{max}}\Delta\nu_{1/2}) / (G\nu_{\text{max}}R^2)]$ with $G = 2$ and $R = 5.0$ Å. ^d Reorganization energy, calculated from $E_{\text{op}} = \lambda_{\text{fc}} + \Delta E_o$, with E_{op} = observed energy of the MMCT band.

Magnetism. The magnetic moments at room temperature of all complexes containing a central Fe(III)Pc unit were determined (for details, see Experimental Section). The measurements are tabulated in the Supporting Information. The Fe(III) center

(23) Goldsberg, K. A.; Meyer, T. J. *Inorg. Chem.* **1984**, *23*, 3002.

(24) Hush, N. S. *Prog. Inorg. Chem.* **1967**, *8*, 391.

(25) Laidlaw, W. M.; Denning, R. G. *J. Chem. Soc., Dalton Trans.* **1994**, 1987.

(26) Sato, M.; Hayashi, Y.; Kumakura, S.; Shimizu, N.; Katada, M.; Kawata, S. *Organometallics* **1996**, *15*, 721.

Table 5. Parameters of ^{57}Fe Mössbauer Spectra of [3Ba]SbF₆^a

<i>T</i> (K)	subpectrum	$\delta^{\alpha\text{-Fe}}$ (mm s ⁻¹) ^b	Γ (mm s ⁻¹) ^c	ΔE_Q (mm s ⁻¹) ^d	Γ_2/Γ_1 ^e	<i>A_r</i> (%; <i>A/A_Σ</i>) ^f	<i>A₂/A₁</i> ^g	<i>F</i> ^h
380(2)	I	+0.04	0.26	1.99	1.05	64	1.18	0.98
	II	+0.25	0.45	0.34	0.47	36	0.35	
295(3)	I	+0.08	0.25	2.03	1.13	93	1.01	1.12
	II	+0.23	0.32	0.33	1.00 ⁱ	7	1.00 ⁱ	
235(3)	I	+0.12	0.26	2.03	1.22	100	1.05	1.04
187(4)	I	+0.13	0.29	2.03	1.34	100	1.00	1.06
135(3)	I	+0.15	0.39	2.04	1.84	100	1.06	1.05
77(2)	I	+0.13	0.76	2.04	2.8	100	1.04	1.22

^a Asymmetrical doublets were used for the fit, except for the symmetrical subpectrum II at 295 K. ^b Isomer shift referred to $\alpha\text{-Fe}$ at room temperature. ^c Full width at half-height. ^d Quadrupole splitting. ^e Asymmetry parameter of the doublet with respect to the line widths of both lines. Γ_1 is the left line. ^f Line area relative to total area. ^g Asymmetry parameter of the doublet with respect to the line areas of both lines. ^h Normalized value of the χ^2 test. ⁱ Fixed value.

is the only species with unpaired electrons in the systems, and due to the presence of the Pc and CN ligands, it is in the low-spin state. i.e., the spin-only magnetism should correspond to $\mu_{\text{eff}} = 1.73 \mu_{\text{B}}$. All observed magnetic moments are, however, in the 2.20–2.31 μ_{B} range. This corresponds to the observations for other Fe(III) systems with porphyrin or phthalocyanine ligands, which, for all kinds of axial ligands, show magnetic moments of this magnitude resulting from spin–orbit coupling.^{27,28} The peculiar nature of the cyanometal ligands in these systems thus does not alter the intrinsic magnetic properties of the Fe(III)Pc core.

Mössbauer Data. To gain further insight into the spin state and electronic situation, we recorded some Mössbauer spectra of the complexes. For the cyanometal ligand, Cp(dppe)Fe–CN was chosen as a reference compound for the external organometallic Fe(II) units in the cyanide-bridged complexes. Its Mössbauer spectra (for details, see Experimental Section), recorded between 77 and 291 K, show a well-resolved symmetrical quadrupole doublet with $\delta = 0.16$ mm/s and $\Delta E_Q = 1.81$ mm/s at 291 K. This is typical for an Fe(II) compound of low-spin configuration in a ligand field of low symmetry. The *C_s*-symmetrical ligand field of Cp(dppe)FeCN leads to an electric field gradient based on ligand contributions, which results in a sizable quadrupole splitting.^{29,30}

Second, complex [3Ba]SbF₆ was chosen as the species with only Fe(III) in the central position and external Cp(PPh₃)₂Ru units. Its Mössbauer data are listed in Table 5. Its Mössbauer spectra, displayed in Figure 5 as a function of temperature, show two unusual features. At low temperatures, there is a very asymmetrical quadrupole doublet ($\delta = 0.13$ mm/s, $\Delta E_Q = 2.04$ mm/s), while at high temperatures, a major wide doublet ($\delta = 0.04$ mm/s, $\Delta E_Q = 1.99$ mm/s) and a minor narrow doublet ($\delta = 0.25$ mm/s, $\Delta E_Q = 0.34$ mm/s), both asymmetrical, are observed. The narrow doublet grows at temperatures above ca. 250 K. As an explanation for these observations, it can be assumed that at low temperatures there is a low-spin Fe(III) system. The increased asymmetry and line broadening with decreasing temperature in the $S = 1/2$ system is due to a slow spin–lattice relaxation rate at low temperature. The preferential broadening of the higher-energy line suggests that the axial component of the electric field gradient (EFG), V_{zz} , must be

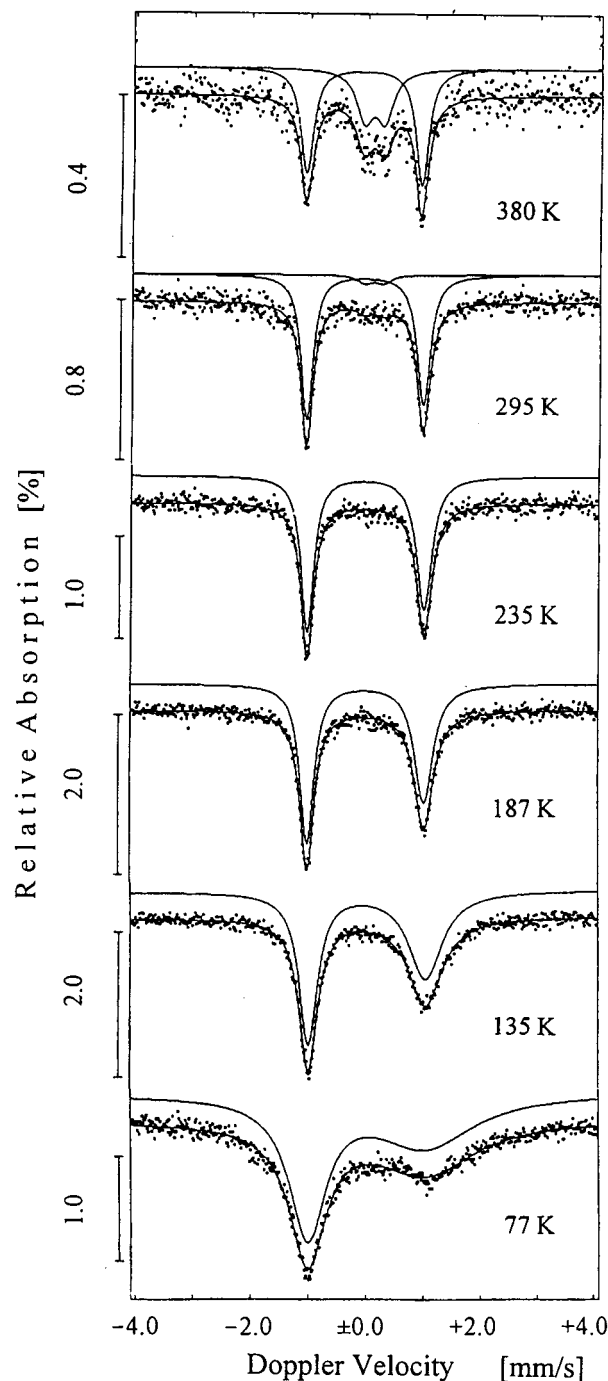


Figure 5. Mössbauer spectra of [3Ba]SbF₆ at varying temperatures. positive, so that the ground state is $(d_{xy})^2(d_{xz}d_{yz})^3$.²⁸ The narrow doublet at high temperatures cannot originate from an Fe(II)Pc

(27) Kalz, W.; Homborg, H.; Küppers, H.; Kennedy, B. J.; Murray, K. S. *Z. Naturforsch.* **1984**, *39b*, 1478.

(28) Kennedy, B. J.; Murray, K. S.; Zwack, P. R.; Homborg, H.; Kalz, W. *Inorg. Chem.* **1986**, *25*, 2539.

(29) Fluck, E. In *Chemical Applications of Mössbauer Spectroscopy*; Goldanskii, V. I., Herber, R. H., Eds.; Academic Press: New York, 1968; Chapter 4, p 268. Kerler, W.; Neuwirth, W. *Z. Phys.* **1962**, *167*, 176.

(30) Kersting, B.; Kolm, M. J.; Janiak, C. *Z. Anorg. Allg. Chem.* **1998**, *624*, 775.

unit produced by a thermally induced intervalence transition between Ru(II) and Fe(III) because its δ and ΔE_Q do not correspond to Fe(II) in such a ligand environment.³¹ Low-spin iron(II) in an octahedral ligand field (O_h symmetry) normally gives a singlet and no quadrupole splitting. Here, the ligand field at the iron center is of local D_{4h} symmetry. For many low-spin iron(II) complexes of the type $[\text{Fe}^{\text{II}}\text{PcL}_2]$, a large quadrupole splitting around 2.0 mm s^{-1} is well documented. A ground state of $(d_{xy})^2(d_{xz}, d_{yz})^3(d_{z^2})^1$ is thereby assumed. This is no real low-spin configuration, so the configuration gives a strong valence contribution to the EFG. Consequently, the quadrupole doublet with a small splitting cannot be due to iron(II) within the picture of an intervalence transition in **[3Ba]**SbF₆. Instead, it must be assumed that the additional doublet originates from a spin crossover equilibrium,³² which, at higher temperatures, favors high-spin Fe(III)Pc for which δ and ΔE_Q are then typical.^{28,30} The well-resolved resonance absorptions for both spin states indicate that the low-to-high-spin relaxation rate must be smaller than 10^7 s^{-1} .

The features of both reference compounds are combined in the Mössbauer spectra of the Fe(II)₂Fe(III) compound **[3Aa]**-SbF₆, and the spectra are displayed in the Supporting Information. The temperature-dependent spectra can be fitted by a major quadrupole doublet (at 380 K $\delta = 0.06 \text{ mm/s}$, $\Delta E_Q = 2.49 \text{ mm/s}$) assigned to Fe(II) in Cp(dppe)Fe, a quadrupole doublet of approximately half intensity (at 380 K, $\delta = 0.12 \text{ mm/s}$, $\Delta E_Q = 1.72 \text{ mm/s}$) assigned to the larger quantity of low-spin Fe(III)Pc, and a small and narrow quadrupole doublet (at 380 K, $\delta = 0.24 \text{ mm/s}$, $\Delta E_Q = 0.44 \text{ mm/s}$) assigned to the smaller quantity of high-spin Fe(III)Pc. Thus, a spin crossover equilibrium exists for the central Fe(III)Pc unit in **[3Aa]**⁺, in which the occurrence of the high-spin component sets in at somewhat lower temperatures than for **[3Ba]**⁺. Some of the enhanced magnetic moments recorded for the trinuclear complexes may be caused by this at room temperature. Altogether, the Mössbauer data confirm the valence-trapped situation and the assignments of the oxidation and spin states used for the interpretation of the redox, MMCT, and magnetic measurements.

Conclusions

Metal–metal interactions along cyanide-linked chains of three metal atoms containing a central redox-active FePc unit were probed by electrochemistry, optical spectroscopy, and Mössbauer measurements, supplemented by preparative redox and magnetic investigations. The electron richness and the accessibility for electron transfer of the various metallic constituents which had previously¹⁹ been checked by $\nu(\text{CN})$ data could be quantified with voltammetric measurements and correlated with the kind and number of the organometallic constituents, the orientation (CN/NC) of the cyanide bridges, and the oxidation state of the central FePc unit. The species containing a central Fe(III)Pc unit exhibit characteristic MMCT bands in their NIR spectra, which correspond to an intervalence transfer from the outer organometallic units to the central Fe(III). Their energies can be correlated in a semiquantitative fashion with the redox properties of the two metallic units involved, which, in turn, are correlated with the orientation of the cyanide bridges. In addition to this short-range MMCT, a long-range metal–metal interaction between the outer organometallic units could be

derived from the cyclic voltammograms of the symmetrical trinuclear complexes displaying a characteristic splitting of their redox waves. Mössbauer data have confirmed the spin- and redox-state assignments and revealed as an additional phenomenon a spin crossover equilibrium above room temperature consisting of a low-spin/high-spin transition of the central Fe(III)Pc units.

In summary, the combined pieces of information allow us to call the complex $[\text{Cp}(\text{dppe})\text{Fe}(\text{II})-\text{CN}-\text{Fe}(\text{III})\text{Pc}-\text{NC}-\text{Fe}(\text{II})-(\text{dppe})\text{Cp}]^+$ an authentic molecular representation of Prussian Blue: it is deeply colored (actually blue, due to the Q-band of the FePc unit), redox-active, and, by having the cyanide nitrogens attached to Fe(III) and the cyanide carbons to Fe(II), the most stable of its three isomers. Moreover, the complex exhibits a MMCT band corresponding to an exchange of the oxidation states between Fe(II) and Fe(III).

Experimental Section

The general experimental procedures are outlined in ref 19, and the details of the voltammetric and spectroscopic measurements are given in ref 16.

Magnetic measurements were performed at room temperature on a Gouy balance for all compounds. The values of χ_{mol} obtained for the paramagnetic complexes were corrected for diamagnetism. For this purpose, the diamagnetic susceptibilities of the corresponding diamagnetic Fe(II)Pc complexes were used when available. The effective magnetic moments were then calculated according to $\mu_{\text{eff}} = 2.828 - (\chi_{\text{mol}}^{\text{corr}})^{1/2}$. Reference measurements were performed using $\text{K}_3[\text{Fe}(\text{CN})_6]$, with $\mu_{\text{eff}} = 2.21 \mu_B$ at room temperature.

Mössbauer Spectroscopy. ⁵⁷Fe Mössbauer spectra were collected in the constant acceleration mode with a triangular velocity profile and were digitized in 1024 data channels. The ⁵⁷Co source in a Rh matrix (AMERSHAM-Buchler) had an activity of about 60 MBq. The Mössbauer transition at 14.41 keV was used for γ -radiation. The transmission of γ -radiation was detected with a NaI(Tl) scintillation counter coupled with a secondary electron multiplier. The experimental spectra were iteratively approximated in a least-squares fit with Lorentz functions in the thin absorber approximation (program package NORMOS).³³ Singlets were fitted with a single Lorentz curve and doublets with a symmetrical or an asymmetrical superposition of two Lorentz functions. The spectral parameters (δ , Γ , and possibly ΔE_Q) could each be fixed or correlated at will in groups in the case of a multiline fit. Largely open parameters were used to aim for fits. The $\delta^{\alpha\text{-Fe}}$ scale of the isomer shift is related to the shift of α -iron as the origin of the ordinate ($\delta^{\alpha\text{-Fe}} = 0.11 \pm 0.01 + \delta^{\text{Fe/Rh}}$, in mm/s).³⁴ The sample was cooled and heated under vacuum to collect the low- and high-temperature spectra.

Chemical Redox Reactions. Oxidations. General Procedure. A solution of the Fe(II)Pc complex in dichloromethane (50 mL) was treated dropwise with stirring with a solution of $[\text{FeCp}_2]\text{SbF}_6$ in dichloromethane (10 mL). After being filtered, the solvent was removed in vacuo, and the residue was washed three times with 20 mL of benzene and dried again in vacuo. It was then taken up in dichloromethane (20 mL) and layered carefully with petroleum ether (bp 60–70 °C). After about 1 week, the hexafluoroantimonate salt of the Fe(III)Pc complex had separated as black needles, which were characterized by IR spectroscopy and cyclic voltammetry.

Complex 3Ac. This reaction has already been described in the preceding paper.¹⁹

Complex 3Ba. Complex **3Ba** was synthesized from 152 mg (0.07 mmol) of **3Ba**·2CH₂Cl₂ and 28 mg (0.07 mmol) of $[\text{FeCp}_2]\text{SbF}_6$, yielding 132 mg (88%) of **[3Ba]**SbF₆.

(31) Hanack, M.; Keppeler, U.; Lange, A.; Hirsch, A.; Dieing, R. In *Phthalocyanines: Properties and Applications*; Leznoff, C. C., Lever, A. B. P., Eds.; VCH: Weinheim, Germany, 1993; Vol. 2, pp 43–96.
(32) Gütllich, P.; Hauser, A.; Spierer, H. *Angew. Chem.* **1994**, *106*, 2109; *Angew. Chem., Int. Ed. Engl.* **1994**, *33*, 2024.

(33) Brand, R. A. *NORMOS*; University of Duisburg: Distribution through Wissel, Starnberg, Germany, 1992.
(34) Stevens, J. G.; Gettys, W. L. Mössbauer Isomer Shifts. In *Mössbauer Isomer Shift Reference Scales*; Shenoy, G. F., Wagner, F. E., Eds.; North-Holland Publishers: Amsterdam, 1978; p 903.

Complex 3Bb. Complex **3Bb** was synthesized from 189 mg (0.09 mmol) of **3Bb** and 40 mg (0.09 mmol) of [FeCp₂]SbF₆, yielding 190 mg (90%) of [3Bb]SbF₆.

Complex [2A]⁻. Complex [2A]⁻ was synthesized from 113 mg (0.08 mmol) of [CoCp₂][2A]·CH₂Cl₂ (see below) and 31 mg (0.08 mmol) of [FeCp₂]SbF₆, yielding 59 mg (65%) of **2A**.

Complex [2B]⁻. Complex [2B]⁻ was synthesized from 100 mg (0.06 mmol) of [CoCp₂][2B]·2CH₂Cl₂ (see below) and 24 mg (0.06 mmol) of [FeCp₂]SbF₆, yielding 59 mg (75%) of **2B**.

Reductions. General Procedure. A solution of the Fe(III)Pc complex in dichloromethane (50 mL) was treated dropwise with stirring with a solution of CoCp₂ in dichloromethane (10 mL). The reaction mixture was kept in a refrigerator for 1 day, during which the Fe(II)Pc complex precipitated as a microcrystalline material characterized by IR spectroscopy and cyclic voltammetry.

Complex 2x. Complex **3Ba** was synthesized from 512 mg (0.23 mmol) of [3Ba]SbF₆ and 43 mg (0.23 mmol) of CoCp₂, yielding 420 mg (85%) of **3Ba**·2CH₂Cl₂.

Complex 2x. Complex **3Bb** was synthesized from 300 mg (0.13 mmol) of [3Bb]SbF₆ and 25 mg (0.13 mmol) of CoCp₂, yielding 210 mg (78%) of **3Bb**.

Complex 2x. Complex [2A]⁻ was synthesized from 203 mg (0.18 mmol) of **2A** and 38 mg (0.20 mmol) of CoCp₂. The raw product was washed three times with 10 mL of benzene and dried in vacuo again. Then it was taken up in 60 mL of dichloromethane and layered carefully with petroleum ether (bp 60–70 °C). After a few days, 198 mg (79%)

of [CoCp₂][2A]·CH₂Cl₂ had precipitated as a dark green powder (mp 215 °C dec).

Anal. Calcd for C₇₆H₅₇Cl₂CoFeN₁₀P₂ (*M_r* = 1413.83): C, 64.56; H, 4.06; N, 9.91. Found: C, 63.87; H, 3.92; N, 10.70.

IR (CH₂Cl₂): $\tilde{\nu}$ (CN) at 2064(w) and 2081(m) cm⁻¹.

Complex 2x. Complex [2B]⁻ was synthesized like **2A** but with 200 mg (0.15 mmol) of **2B** and 32 mg (0.17 mmol) of CoCp₂, yielding 197 mg (77%) of [CoCp₂][2B]·2CH₂Cl₂ as a dark green powder (mp 220 °C dec).

Anal. Calcd for C₈₇H₆₅Cl₄CoFeN₁₀P₂Ru (*M_r* = 1670.15): C, 62.15; H, 3.67; N, 8.30. Found: C, 62.57; H, 3.92; N, 8.37.

IR (CH₂Cl₂): $\tilde{\nu}$ (CN) at 2084(w) and 2113(m) cm⁻¹.

Acknowledgment. This work was supported by the Graduiertenkolleg "Ungepaarte Elektronen" of the Deutsche Forschungsgemeinschaft. The authors thank Prof. J. Heinze and co-workers and Dr. Nianrong Zhu for assistance during the measurements and interpretation.

Supporting Information Available: Figures showing a comparison of the MMCT spectra of [3Aa]⁺ and [3Ba]⁺ and the variable-temperature Mössbauer spectra of [3Aa]SbF₆ and a tabulation of the magnetic measurements of all complexes containing a central Fe(III) unit. This material is available free of charge via the Internet at <http://pubs.acs.org>.

IC000096Y